

## High-Resolution $^7\text{Li}$ Solid-State NMR Study of $\text{Li}_x\text{V}_2\text{O}_5$ Cathode Electrodes for Li-Rechargeable Batteries

Riqiang Fu,<sup>\*,†</sup> Zhiru Ma,<sup>†,‡</sup> Jim P. Zheng,<sup>§</sup> G. Au,<sup>||</sup> E. J. Plichta,<sup>||</sup> and Chaohui Ye<sup>#</sup>

Center for Interdisciplinary Magnetic Resonance, National High Magnetic Field Laboratory, 1800 E. Paul Dirac Drive, Tallahassee, Florida 32310, Department of Electrical and Computer Engineering, Florida A&M University and Florida State University, Tallahassee, Florida 32310, U.S. Army Communications-Electronics Command, Ft. Monmouth, New Jersey 07703, and Wuhan Institute of Physics and Mathematics, the Chinese Academy of Sciences, Wuhan 430071, P. R. China

Received: April 24, 2003; In Final Form: July 1, 2003

The  $\text{Li}_x\text{V}_2\text{O}_5$  cathode of Li-rechargeable battery cells under three different charge states have been studied by high-resolution solid-state  $^7\text{Li}$  magic angle spinning (MAS) NMR spectroscopy. In the charged and discharged states, three different  $^7\text{Li}$  NMR resonances, corresponding to the  $\text{Li}^+$  ions in the electrolyte, in the  $\text{V}_2\text{O}_5$  cathode, and on the surface of the  $\text{V}_2\text{O}_5$  cathode, were identified by their spin–lattice relaxation times in inversion recovery experiments. Only signals of the  $\text{Li}^+$  ions in the electrolyte were observed in the over charged state. It is shown experimentally that the  $\text{Li}^+$  ions in the electrolyte experience a dynamics or exchange process in a time scale of milliseconds with those in the  $\text{V}_2\text{O}_5$  cathode, in particular for the discharged state, where a severe cross relaxation effect was observed in the inversion recovery for the  $\text{Li}^+$  ions in the electrolyte. It is concluded that such an exchange is mediated by the  $\text{Li}^+$  ions on the surface of the  $\text{V}_2\text{O}_5$  cathode. Therefore, the surface structure of the  $\text{V}_2\text{O}_5$  cathode electrode plays an important role in the reversibility of the  $\text{Li}^+$  ions in the rechargeable battery.

### Introduction

In the past several decades, studies of electrode materials used for lithium rechargeable batteries have received considerable attention because of important scientific and technological applications of the materials. Lithium rechargeable batteries consist of an anode (e.g., metallic lithium and lithiated carbons), lithium-ion conducting electrolyte, and a lithium insertion cathode such as  $\text{Li}_x\text{V}_2\text{O}_5$  and  $\text{Li}_{1+x}\text{CoO}_2$ .<sup>1,2</sup> During discharge process,  $\text{Li}^+$  ions move from the anode via the electrolyte to the host structure of the cathode. The  $\text{Li}^+$  ions are extracted from the cathode and migrate back to the anode through the electrolyte during charge process. Thus, electrochemical stability of the anode, electrolyte, and cathode materials during the charge–discharge cycles is key to the lifetime of the batteries.

Numerous techniques have been employed to understand the mechanism of the battery capacity degradation. Traditional electrochemical methods such as the charge–discharge cycles and ac impedance spectroscopy demonstrated a relationship between the capacity degradation and the increasing resistance of the battery. For instance, the depletion of organic electrolytes<sup>3,4</sup> and the deposition of lithium<sup>5</sup> and other films<sup>4</sup> on the electrode surfaces during charge–discharge cycles increased the battery impedance and ultimately resulted in the ending of the batteries. X-ray diffraction and transmission electron microscope (TEM) indicated that the charge–discharge cycles caused

microstructural damage and cation disorder of the oxide electrodes.<sup>6,7</sup> Nuclear magnetic resonance (NMR) spectroscopy has also been used to evaluate immediate structural and electronic environments of  $\text{Li}^+$  and other ions in a variety of the host materials for both crystalline and amorphous phases. Many NMR studies have focused on the anode materials to understand the effect of carbon structure and morphology on the reversibility of the  $\text{Li}^+$  ions. There are different lithium electronic environments in the battery such as Li dendrites and Li intercalated in carbon used as an anode,<sup>8,9</sup> distinct portions for the reversible and irreversible Li,<sup>8</sup> and the covalently bonded and metallic Li.<sup>10</sup> It has been well known that  $^7\text{Li}$  NMR is extremely sensitive to the lithium chemical shift environments. For example, even a small fraction of the excess Li and impurities in the  $\text{LiCoO}_2$  cathode was visible in  $^7\text{Li}$  NMR spectra.<sup>11,12</sup> For the  $\text{V}_2\text{O}_5$  cathode, it was shown<sup>13–16</sup> that there were different  $\text{Li}_x\text{V}_2\text{O}_5$  phases ( $\alpha$ ,  $\epsilon$ ,  $\delta$ , and  $\gamma$ ) depending on the  $\text{Li}^+$  ions concentration when lithium ions were intercalated into the  $\text{V}_2\text{O}_5$  by chemical and electrochemical methods.

In this work, high-resolution  $^7\text{Li}$  solid-state NMR spectroscopy is used to study the electronic environments of  $\text{Li}_x\text{V}_2\text{O}_5$  cathodes from Li-rechargeable battery cells at charged, discharged, and over cycled states. By comparing  $^7\text{Li}$  chemical shifts in the three charged states, we further discuss the mechanism of the capacity degradation of the battery.

### Materials and Experiments

Panasonic vanadium pentoxide ( $\text{V}_2\text{O}_5$ ) lithium-rechargeable batteries (part No. VL2320-1HF) were purchased and used in our experiments. These “button” battery cells are 23 mm in diameter and 2.0 mm in thickness with a structural arrangement of Li (anode)/membrane (electrolyte)/ $\text{V}_2\text{O}_5$  (cathode). An aluminum mesh and a stainless steel bottom case of the button

\* Corresponding author. E-mail: rfu@magnet.fsu.edu; fax: (850)644–5044.

<sup>†</sup> Center for Interdisciplinary Magnetic Resonance.

<sup>‡</sup> Present address: Department of Chemistry, University of Utah, Salt Lake City, UT 84112.

<sup>§</sup> Florida A&M University and Florida State University.

<sup>||</sup> U.S. Army Communications-Electronics Command.

<sup>#</sup> The Chinese Academy of Sciences.

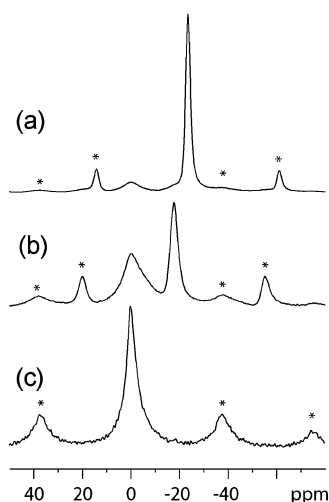


**Figure 1.**  ${}^7\text{Li}$  MAS NMR spectra of  $\text{Li}_x\text{V}_2\text{O}_5$  cathode materials from three different charge states: (a) discharged state, (b) charged state, and (c) over cycled state. The asterisks indicate the spinning sidebands.

cell were used as current collectors for the anode and cathode, respectively. Physical and chemical properties of the cathode material were analyzed by high-resolution TEM, selected area electron diffraction (SAED), and energy-dispersive X-ray spectroscopy (EDX). Our TEM images indicated that the cathode contained both crystalline and amorphous phases.<sup>17</sup> The majority was formed with large particles in the order of  $\mu\text{m}$ , which were in a single crystalline phase of  $\text{Li}_x\text{V}_2\text{O}_5$ , close to the crystal structure of  $\text{V}_2\text{O}_5$ , as suggested by the SAED patterns, while the amorphous phase contained small particles. The EDX analyses indicated that the amorphous region contained a high amount of Al. Besides V and Al, no other element heavier than oxygen was found in the cathode.

An Arbin battery test system was used to charge and discharge the battery cells. A button cell was charged to 3.4 V at a constant voltage mode of 3.4 V (i.e., the charged state), another cell was discharged to 2.1 V at a constant current mode at 10 mA (i.e., the discharged state), and the third one was charged and discharged repeatedly until the battery cell was dead (i.e., the over cycled state). The three cells were opened under an argon atmosphere in a glovebox where the  $\text{Li}_x\text{V}_2\text{O}_5$  cathodes were removed from the cells and then packed into three different MAS rotors for NMR studies.

The  ${}^7\text{Li}$  NMR measurements were performed on a Bruker DMX-600 NMR spectrometer ( $B_0 = 14.1$  T) with a  ${}^7\text{Li}$  Larmor frequency of 233.31 MHz using a 4-mm Bruker double-resonance MAS NMR probe. Inversion recovery  $T_1$  measurements were carried out at various temperatures, which were controlled within  $\pm 0.1$  K by a Bruker BVT-2000 unit. A set of 32 spectra with different recovery times was used for each  $T_1$  measurement and eight scans were accumulated for each spectrum with a recycle delay of 2 s. The samples were spun at 8.6 kHz during the experiments. A 1 M aqueous LiCl was used as an external chemical shift reference (0 ppm).

## Results and Discussion

Figure 1 shows the  ${}^7\text{Li}$  MAS NMR spectra for the  $\text{Li}_x\text{V}_2\text{O}_5$  samples at the different charged states. Clearly, there exists a broad peak at  $-0.4$  ppm in the spectra. For the discharged state, the resonance at  $-23.6$  ppm has much greater intensity than that at  $-0.4$  ppm and thus can be attributed to the excess  $\text{Li}^+$  ions inserted into the  $\text{Li}_x\text{V}_2\text{O}_5$  cathode electrode during the discharge process. For the charged state, the peak intensity at

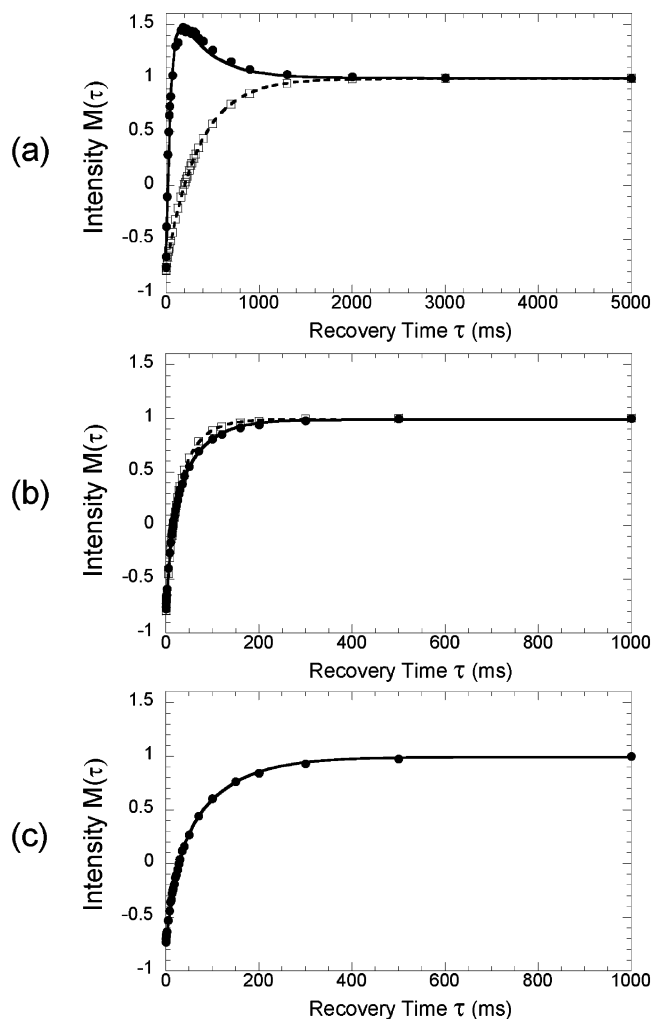


**Figure 2.** Plots of  ${}^7\text{Li}$  signal intensities  $M(\tau)$  of the  $\text{Li}_x\text{V}_2\text{O}_5$  cathode as a function of recovery time  $\tau$  under different charge states: (a) discharged state, (b) charged state, and (c) over cycled state. All of the experimental data were recorded on a Bruker DMX600 NMR spectrometer at 300 K and normalized to their equilibrium magnetizations. The solid circles and the squares indicate the signal intensities integrated from  $-8$  to  $+8$  ppm and from  $-15$  ppm to  $-30$  ppm, corresponding to the chemical shifts of the  $\text{Li}^+$  ions in the electrolyte and in the cathode, respectively. In Figure 2a, eq 1 was used to fit the solid circles as indicated by the solid line and a single-exponential component was applied for the squares (cf. the dashed line). All the data in Figure 2b and c were fitted using two exponential components.

$-17.6$  ppm is on the same order of that at  $-0.4$  ppm. For the over cycled state, no resonance peak is observed between  $-15.0$  and  $-30.0$  ppm. In fact,  ${}^{51}\text{V}$  NMR measurements also indicated that the concentration of the  $\text{Li}^+$  ions in the over cycled  $\text{Li}_x\text{V}_2\text{O}_5$  cathode electrode was so low that the  $\text{V}^{5+}$  species was predominate.<sup>18</sup> Therefore, it is believed that the chemical shifts of the  $\text{Li}^+$  ions in the  $\text{Li}_x\text{V}_2\text{O}_5$  cathode are in the range between  $-15.0$  and  $-30.0$  ppm.

Figure 2 shows the inversion recovery of the  ${}^7\text{Li}$  magnetization from the three charged states. For the discharged state, the signals integrated from  $-15.0$  to  $-30.0$  ppm, which corresponds to the chemical shift range for the  $\text{Li}^+$  ions in the cathode, follows a single-exponential inversion recovery curve with a spin-lattice relaxation time  $T_1$  of  $344.5 \pm 2.1$  ms. This is consistent with the predominate  $\text{Li}^+$  ions in the cathode. However, the signals integrated from  $8.0$  to  $-8.0$  ppm, a chemical shift range for the  $\text{Li}^+$  ions outside the cathode, apparently overshoots to a maximum above the equilibrium value and then slowly decays back to the equilibrium. Such a

**TABLE 1:**  ${}^7\text{Li}$  Spin–Lattice Relaxation Time of the  $\text{Li}_x\text{V}_2\text{O}_5$  Cathode at Different Charge States<sup>a</sup>

samples	$T_1^E$		$T_1^S$ (ms)	$T_1^C$ (ms)	$T_1^C$ (ms)
	0 ppm	−4.0 ppm	at −17.0 ppm	at −21.0 ppm	at −23.6 ppm
discharged state	49.0 ± 2.1				344.5 ± 2.1
charged state	57.3 ± 2.7	10.6 ± 0.7	13.8 ± 1.7	41.6 ± 3.0	
over cycled state	95.0 ± 4.9				
	20.2 ± 1.7				

<sup>a</sup> In this Table,  $T_1^E$ ,  $T_1^S$ , and  $T_1^C$  represent the spin–lattice relaxation time for the  $\text{Li}^+$  ions in the electrolyte, on the surface of the cathode, and in the  $\text{Li}_x\text{V}_2\text{O}_5$  cathode, respectively.

phenomenon was observed in solution NMR<sup>19</sup> as well as in some solid-state systems<sup>20–22</sup> because of the heteronuclear transient nuclear Overhauser effect (NOE). However, to the best of our knowledge, this phenomenon has not been reported for homonuclear systems in the literature. Since the magnetization relaxes from the maximum to the equilibrium at a time constant of  $\sim 345$  ms, which is the same as the  $T_1$  value of the  $\text{Li}^+$  ions in the cathode, it is believed that the excess  $\text{Li}^+$  ions in the cathode affect relaxation behavior of the  $\text{Li}^+$  ions outside the cathode (i.e., in the residual electrolyte). In other words, there exists cross relaxation or exchange between the  $\text{Li}^+$  ions in the cathode and those in the residual electrolyte.

For heteronuclear systems, the cross relaxation rate from dilute spins (e.g.,  ${}^{13}\text{C}$ ) to abundant spins (e.g.,  ${}^1\text{H}$ ) is much smaller than that from the abundant spins to the dilute spins because of low natural abundance for the dilute spins (e.g., 1.1% for  ${}^{13}\text{C}$ ),<sup>23</sup> so that the cross relaxation severely affects the relaxation behavior of the dilute spins.<sup>20–22</sup> For the homonuclear system studied here, the signal intensity at −23.6 ppm is much greater than that at −0.4 ppm, indicating that there are much more  $\text{Li}^+$  ions in the cathode than in the residual electrolyte. In analogies to the analysis for the heteronuclear systems,<sup>20–22</sup> the magnetization at around −0.4 ppm during the inversion recovery can be described by

$$M(\tau) = 1 - (1 + k)\exp(-\tau/T_1^E) + \frac{T_1^E}{T_1^{\text{EC}}}(1 + k)[\exp(-\tau/T_1^C) - \exp(-\tau/T_1^E)] \quad (1)$$

where  $T_1^E$  and  $T_1^C$  are the spin–lattice relaxation times for the  $\text{Li}^+$  ions in the electrolyte and in the cathode, respectively,  $T_1^{\text{EC}}$  stands for the cross relaxation time, and  $k$  is the inversion efficiency. Solid circles in Figure 2a were fitted using eq 1, as indicated by a solid line, where  $T_1^E$ ,  $T_1^{\text{EC}}$ , and  $k$  were treated as variables and  $T_1^C$  was set to 345 ms. The fitting yielded the  $T_1^E$  and  $T_1^{\text{EC}}$  values of  $49.0 \pm 2.1$  and  $86.1 \pm 2.7$  ms, respectively. The  $T_1$  values obtained are listed in Table 1. For both the charged and over cycled states, such a cross relaxation effect was not visible, as in Figure 2b and c. This is because of the lack of the excess  $\text{Li}^+$  ions in the cathode. Instead, the recovery of these signals can be better described by two exponential components. For the charged state, two components obtained from the fittings were  $57.3 \pm 2.7$  and  $10.6 \pm 0.7$  ms for the solid line and  $41.6 \pm 3.0$  and  $13.8 \pm 1.7$  ms for the dashed line (cf. Figure 2b). While for the over cycled state, two components obtained were  $95.0 \pm 4.9$  and  $20.2 \pm 1.7$  ms for the solid line (cf. Figure 2c).

Figure 3 shows the  ${}^7\text{Li}$  spectra taking from the  $T_1$  measurements with an inversion recovery time chosen to identify the signals with different relaxation components. As indicated by arrows in Figure 3, for the discharged and charged states, four resonances can be revealed in the spectra and three out of the four have the same chemical shifts, which are 0, −4.0, and

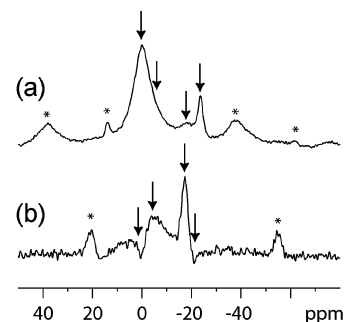


**Figure 3.**  ${}^7\text{Li}$  MAS NMR absorption spectra of the  $\text{Li}_x\text{V}_2\text{O}_5$  cathode materials at different inversion recovery times. (a) The recovery time was 230 ms for the discharged state. (b) The recovery time was set to 18 ms for the charged state. The asterisks indicate the spinning sidebands while the arrows represent the positions of the isotropic chemical shifts.

−17.0 ppm. The fourth signal appearing at −23.6 and −21.0 ppm for the discharged and charged states, respectively, can be assigned to the  $\text{Li}^+$  ions in the cathode.<sup>24</sup> For example, at a given recovery time for the charged state as in Figure 3b, the signal at −17.0 ppm was positive and the signal at −21.0 ppm was still negative, implying that the observed peak at −17.6 ppm (cf. Figure 1b) is in fact superimposed by two resonances at −17.0 and −21.0 ppm with the former having a shorter relaxation time than the latter. On the other hand, the signal at −4.0 ppm became positive at the given recovery time while the signal at 0 ppm remained negative, indicating that the broad peak at around −0.4 ppm (cf. Figure 1) is superimposed by two chemical shifts positioning at 0 and −4.0 ppm, as indicated by the arrows in Figure 3b. For the discharged state, as can be seen in Figure 1a, it seems like there is a small shoulder with a low intensity at around −17.0 ppm. Since it is so close to the intense peak at −23.6 ppm, it is hardly considered to be a resonance signal. However, at a given recovery time when the intense signal at −23.6 ppm was close to null, the signal at −17.0 ppm became clearly visible, as shown in Figure 3a, although its relaxation parameter could not be reliably obtained because its signal intensity was rather small and could hardly be separated from the intense signal at −23.6 ppm for most of the recovery times. While the signal at −4.0 ppm, as indicated by an arrow in Figure 3a, could be identified at another recovery time (spectrum not shown), the solid circles were still fitted using eq 1 without adding an additional relaxation component. For the over cycled state, no additional resonance can be revealed through this process although there exists two different relaxation components. This implies that the peak is either associated with biexponential relaxation behavior or simply comprised of two resonances with virtually identical chemical shifts. All of the  $T_1$  values for those components obtained through the fittings are summarized in Table 1.

When the battery cell was discharged to 2.1 V, the  $x$  in the cathode was about 1.6 ~ 1.8, which was in a mixture of  $\delta$ - and  $\gamma$ - phases of  $\text{Li}_x\text{V}_2\text{O}_5$ , as defined by Pecquenard et al.<sup>13</sup>

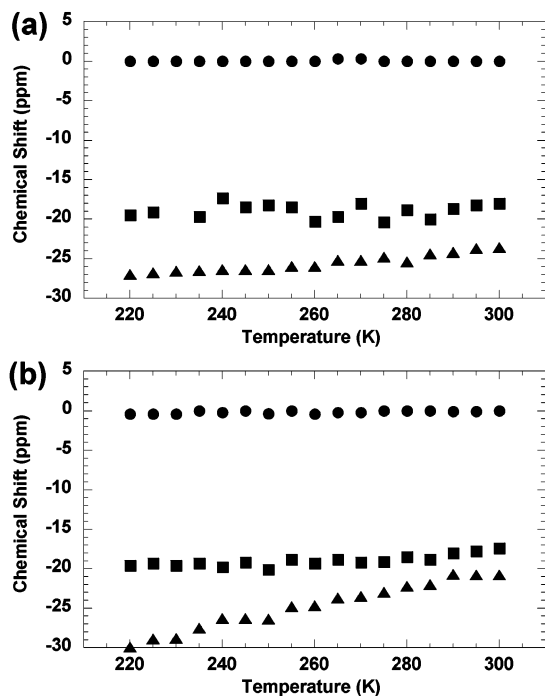


**Figure 4.** Temperature dependence of the  $^7\text{Li}$  chemical shifts for the  $\text{Li}_x\text{V}_2\text{O}_5$  cathode materials at (a) the discharged and (b) the charged states.

Thus, the signal at  $-23.6$  ppm is assigned to the excess  $\text{Li}^+$  ions in the  $\text{Li}_x\text{V}_2\text{O}_5$  cathode because of the great signal intensity. With the high concentration of the  $\text{Li}^+$  ions in the bulk of the  $\text{Li}_x\text{V}_2\text{O}_5$  cathode, the paramagnetic  $\text{V}^{3+}$  and  $\text{V}^{4+}$  species become dominant so that it is relatively difficult to observe the  $^{51}\text{V}$  signals.<sup>18</sup> Figure 4 shows the temperature dependence of the chemical shifts identified in the discharged and charged states. Clearly, it can be seen in Figure 4a that the chemical shift of the excess  $\text{Li}^+$  ions changes almost linearly from  $-23.6$  to  $-27.2$  ppm as the temperature decreases from 300 to 220 K while the signals at  $-0.4$  and  $-17.0$  ppm are nearly temperature independent. It has been known that the chemical shifts of the  $\text{Li}^+$  ions close to the paramagnetic species resulted from a localized paramagnetic interaction and thus are expected to be temperature dependent.<sup>11</sup> When the battery cell was charged to 3.4 V, the  $x$  in the  $\text{Li}_x\text{V}_2\text{O}_5$  cathode was believed to be  $\sim 0.1$ , which was in a mixture of  $\alpha$ - and  $\epsilon$ - phases of  $\text{Li}_x\text{V}_2\text{O}_5$ , again by Pecquenard et al.<sup>13</sup> Similarly, the component whose chemical shift moves from  $-21.0$  to  $-29.7$  ppm as the temperature decreases from 300 to 220 K is attributed to the  $\text{Li}^+$  ions in the  $\text{V}_2\text{O}_5$  host that are localized to the paramagnetic  $\text{V}^{3+}$  or  $\text{V}^{4+}$  species. This implies that there still exists a small amount of the  $\text{Li}^+$  ions in the  $\text{Li}_x\text{V}_2\text{O}_5$  cathode after the charge process, which is consistent with the results obtained by Pecquenard et al.<sup>13</sup> that a small residual of  $\epsilon$ - $\text{Li}_x\text{V}_2\text{O}_5$  ( $x \sim 0.05$ ) remained in the cathode after deintercalation. It is worth noting from Figure 4 that the slope of the temperature-dependent chemical shift for the charged state is greater than that for the discharged state, probably implying that the bonding states of the  $\text{Li}^+$  ions to the  $\text{V}_2\text{O}_5$  host structure are different. In fact, it is reasonable to assume that a small amount of the residual  $\text{Li}^+$  ions after the charge process is primarily localized to the paramagnetic  $\text{V}^{4+}$  species and the excess  $\text{Li}^+$  ions after the discharge process are localized to both the paramagnetic  $\text{V}^{3+}$  and  $\text{V}^{4+}$  species.

On the other hand, the signal at  $-17.0$  ppm is almost temperature independent, as shown in Figure 4, for both the charged and discharged states, regardless of the significant

difference in the  $\text{Li}^+$  ions concentration in the bulk of the  $\text{V}_2\text{O}_5$  host. This resonance peak cannot be from Li-metal because the Knight shift for metallic lithium is typically in the range of  $250\sim 360$  ppm.<sup>25,26</sup> While the signal at  $-17.0$  ppm has similar intensity with respect to the peak intensity at  $-0.4$  ppm for both the charged and discharged states, it is thus attributed to the  $\text{Li}^+$  ions on the surface of the  $\text{V}_2\text{O}_5$  host, since it is reasonable to believe that the  $\text{V}_2\text{O}_5$  hosts in the different charge states have similar surface area.

Although a single  $T_1$  relaxation component was typically observed in gel electrolytes,<sup>27</sup> the broad peak at  $-0.4$  ppm in Figure 1, initially assigned to the  $\text{Li}^+$  ions in the residual electrolyte, contains two relaxation components for all of the three samples used here. For the discharged and charged samples, two different chemical shifts (i.e., 0 and  $-4.0$  ppm) can be revealed via the inversion recovery measurements. A possible explanation is that a small amount of the  $\text{Li}^+$  ions in the electrolyte is close to the surface of the  $\text{V}_2\text{O}_5$  cathode so that those  $\text{Li}^+$  ions have slightly different electronic environment compared to others in the electrolyte. In fact, it was evident that the base of the  $^7\text{Li}$  NMR peak of the gel electrolytes was very broad probably indicating that there existed two different Li electronic environments in the electrolyte, though a single component was used in the  $T_1$  measurements.<sup>27</sup> Since the  $^7\text{Li}$  NMR of the electrolyte of these batteries has a narrow peak at 0 ppm,<sup>18</sup> the signal at  $-4.0$  ppm revealed in the charged and discharged states indeed suggests an existence of additional  $\text{Li}^+$  ion chemical environment between the electrolyte and the surface of the cathode, which should be sensitive to the surface environment of the cathode. For the over cycled state where the surface environment should be largely different from that in the charged or discharged state, no signal is observed at  $-4.0$  ppm.

To confirm the existence of the cross relaxation between the  $\text{Li}^+$  ions in the residual electrolyte and those in the cathode, a two-dimensional NOESY experiment<sup>28</sup> was performed. Figure 5a shows a modified NOESY pulse sequence in which an inversion recovery is incorporated before the standard NOESY experiment.<sup>28</sup> As we have known, in the presence of a very strong signal, it is extremely difficult (or impossible) to observe a very weak cross-peak between the strong signal and a weak signal because of the dynamic range of the digitization. The incorporation of the inversion recovery before the NOESY experiment allows us to prepare the initial magnetization via spin-lattice relaxation times in such a way that the strong signal at  $-23.6$  ppm has a similar intensity as the weak signal at  $-0.4$  ppm. Figure 5b shows the presence of a cross-peak between resonance at 0 ppm and at  $-23.6$  ppm, as indicated by an arrow. Although the cross-peak is weak, its existence suggests that the  $\text{Li}^+$  ions in the residual electrolyte are effectively in close proximity with those intercalated into the cathode.

Table 2 lists the  $^7\text{Li}$  NMR line widths at the half-height of the broad peak at  $-0.4$  ppm for the three samples at different temperatures. Clearly, at 300 K, the  $^7\text{Li}$  line width for the discharged and charged states is much broader than that for the over cycled state. Assuming that the signal at  $-4.0$  ppm for the discharged state has a similar relaxation property as that for the charged state, the diagonal peak at 0 ppm in Figure 5b would receive little contribution from the signal at  $-4.0$  ppm because the mixing time of 80 ms used in the NOESY experiment was much longer than the  $T_1$  value of 10.6 ms so that the signal at  $-4.0$  ppm was completely decayed. The measured line width at the half-height from a slice taken at 0 ppm along the  $\omega_2$  dimension was 1510 Hz, which is also much

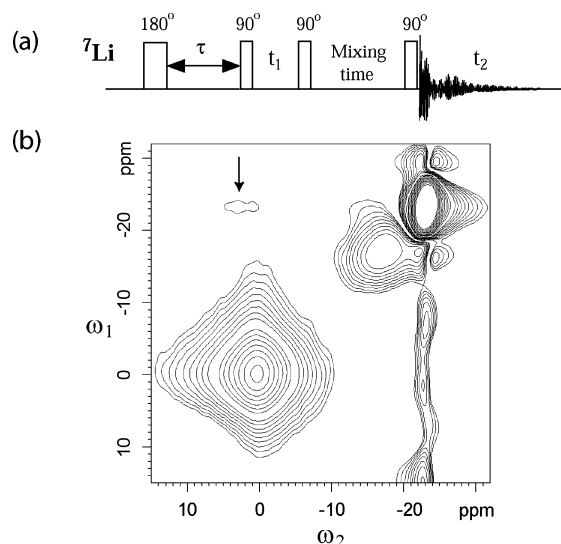


**Figure 5.** (a) A modified pulse sequence for two-dimensional (2D) NOESY experiments. The insertion of the inversion recovery before the standard 2D NOESY experiments is to prepare initial magnetizations via spin–lattice relaxation times  $T_1$  in such a way that the intense signals become the same order as the weak signals so that the weak cross-peaks between them can be observed in the resulting 2D NOESY spectrum. (b)  $^7\text{Li}$  2D NOESY NMR spectrum of the  $\text{Li}_x\text{V}_2\text{O}_5$  cathode at the discharged state. The arrow indicates the cross-peak between 0 and  $-23.6$  ppm. In this experiment, the inversion recovery time  $\tau$  was set to 216 ms to select the maximum magnetization for the signals at around 0 ppm, though the signals at around  $-23$  ppm were still negative. The mixing time used in the experiment was 80 ms. The NOESY experiment was performed at 300 K.

**TABLE 2: Temperature Dependence of the  $^7\text{Li}$  NMR Line Width at the Half-Height of the Signal at around  $-0.4$  ppm for the  $\text{Li}_x\text{V}_2\text{O}_5$  Cathode at Different Charge States**

temperature (K)	line width at half-height (Hz)		
	discharged state	charged state	over cycled state
300	2050	3350	610
220	2030	2200	

broader than the line width of the signal at 0 ppm for the over cycled state (cf. 610 Hz). Thus, broadening of the peak is not solely due to the overlap of the two chemical shifts at 0 and  $-4.0$  ppm, though such an overlap gives rise to a different reading of the chemical shift ( $-0.4$  ppm rather than 0 ppm as in Figure 1). Interestingly, when the temperature was decreased from 300 to 220 K, the line width was decreased slightly from 2050 to 2030 Hz for the discharged state and greatly decreased from 3350 to 2200 Hz for the charged state. Therefore, it can be concluded that the  $\text{Li}^+$  ions in the electrolyte (i.e., the chemical shift at 0 ppm) experience a dynamic or exchange process at 300 K with those in the cathode, as described by<sup>29</sup>

$$\nu_{ic} \sim |\delta_E - \delta_C| \quad (2)$$

where  $\delta_E$  is the chemical shift of the  $\text{Li}^+$  ions in the electrolyte (i.e., 0 ppm),  $\delta_C$  refers to the chemical shifts of the  $\text{Li}^+$  ions in the cathode electrode (i.e.,  $-23.6$  and  $-21.0$  ppm for the discharged and charged states, respectively), and  $\nu_{ic}$  stands for the exchange rate between the  $\text{Li}^+$  ions in the two different chemical environments. Since the two chemical shifts are separated by  $\sim 5000$  Hz, the exchange rate  $\nu_{ic}$  is about a few thousands hertz. As a result, the  $^7\text{Li}$  resonance of the residual electrolyte becomes significantly broad.<sup>29</sup>

Since the  $\text{Li}^+$  ions on the surface of the  $\text{V}_2\text{O}_5$  cathode physically separate the  $\text{Li}^+$  ions in the electrolyte from those in

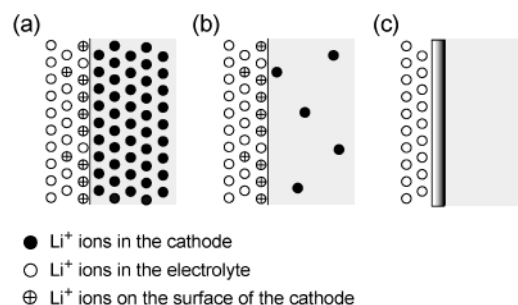


**Figure 6.** Schematic representation of the distribution of the  $\text{Li}^+$  ions in the Li-rechargeable battery cell. (a) Discharged state; (b) charged state; and (c) over cycled state. The  $\text{V}_2\text{O}_5$  cathode is on the right side, as shown in shadowed area, and the electrolyte is on the left side, separated by a surface area as indicated by a solid line or strip. For the discharged and charged states, the  $\text{Li}^+$  ions in the electrolyte and on the surface of the cathode exhibit a thermal dynamics equilibrium, while for the over cycled state, no  $\text{Li}^+$  ions are present on the surface of the cathode.

the  $\text{V}_2\text{O}_5$  host, they act as a mediator between the  $\text{Li}^+$  ions in the two different chemical environments. Figure 6 shows schematic representation of the distribution of the  $\text{Li}^+$  ions in the electrolyte and the  $\text{V}_2\text{O}_5$  cathode. For the discharged state, the  $\text{Li}^+$  ions are saturated on the surface area of the cathode and established a thermal dynamic equilibrium with the  $\text{Li}^+$  ions in the electrolyte, while there exist the excess  $\text{Li}^+$  ions in the  $\text{V}_2\text{O}_5$  cathode so that the  $\text{Li}^+$  ions in the cathode are in close proximity with those on the surface, even if the temperature is low. As a result, the exchange rate remains more or less unchanged in the given temperature range, thus giving rise to a similar line width. Similarly, for the charged state, the  $\text{Li}^+$  ions are saturated on the surface area of the cathode and reached a thermal dynamic equilibrium with the  $\text{Li}^+$  ions in the electrolyte. However, the concentration of the  $\text{Li}^+$  ions in the bulk of the  $\text{V}_2\text{O}_5$  is so low that only a few  $\text{Li}^+$  ions are close to the surface. At room temperature, these  $\text{Li}^+$  ions are still effectively in close proximity with the  $\text{Li}^+$  ions on the surface because they can diffuse easily from one place to another in the  $\text{V}_2\text{O}_5$  cathode, resulting in the broadening of the signal because of the cross relaxation effect, though such an effect is not observed in the inversion recovery curve because of the low concentration of the  $\text{Li}^+$  ions in the cathode (cf. Figure 2b). When the temperature is decreased to 220 K, the  $\text{Li}^+$  ions in the bulk of the cathode become relatively difficult to move so that they have a very limited contact with the  $\text{Li}^+$  ions on the surface. Consequently, the dynamic process between the  $\text{Li}^+$  ions in the electrolyte and those in the  $\text{V}_2\text{O}_5$  host is slowed so that the resonance at 0 ppm becomes significantly narrow at low temperature. Thus, we can reasonably believe that during the discharge process, the  $\text{Li}^+$  ions on the surface of the cathode are moved into the  $\text{V}_2\text{O}_5$  host and at the same time the  $\text{Li}^+$  ions in the electrolyte are moved onto the surface replacing those  $\text{Li}^+$  ions moving into the cathode, as if the  $\text{Li}^+$  ions in the electrolyte are inserted into the cathode. On the other hand, during the charge process, the  $\text{Li}^+$  ions on the surface of the cathode are moved to the electrolyte while the  $\text{Li}^+$  ions in the  $\text{V}_2\text{O}_5$  host are diffused onto the surface replacing those  $\text{Li}^+$  ions moving into the electrolyte, as if the  $\text{Li}^+$  ions are extracted from the cathode to the electrolyte.

For the over charged state, no resonance was observed in the range of  $-15$  to  $-30$  ppm, indicating that there are virtually no  $\text{Li}^+$  ions on the surface of the  $\text{V}_2\text{O}_5$  cathode electrode. As illustrated by the strip in Figure 6c, a thin coat containing no  $\text{Li}^+$  ions effectively separates the cathode and the electrolyte. Therefore, it is reasonable to speculate that the surface structure

of the  $\text{V}_2\text{O}_5$  host is becoming difficult to inhibit the  $\text{Li}^+$  ions during repeated charge–discharge cycles so that the ability for the  $\text{Li}^+$  ions to penetrate through the surface is weakening resulting in the degradation of the battery capacity. In fact, our recent TEM and EDX measurements confirmed that the aluminum of the current collector in the battery cells was deposited on the surface of the  $\text{V}_2\text{O}_5$  cathode electrode during the charge–discharge cycles.<sup>17</sup>

### Conclusion

We have used high-resolution solid-state  $^7\text{Li}$  MAS NMR spectroscopy to study  $\text{Li}_x\text{V}_2\text{O}_5$  cathode at different charge states. In the inversion recovery experiments, we identified three different  $\text{Li}^+$  electronic environments, which are the  $\text{Li}^+$  ions in the electrolyte, in the  $\text{V}_2\text{O}_5$  cathode, and on the surface of the  $\text{V}_2\text{O}_5$  cathode, for the charged and discharged states. For the over cycled state, only the  $\text{Li}^+$  ions in the electrolyte were observed. For the discharged state, the excess  $\text{Li}^+$  ions in the  $\text{V}_2\text{O}_5$  cathode affect the inversion recovery behavior for the  $\text{Li}^+$  ions in the electrolyte through cross relaxation. By observing the  $^7\text{Li}$  NMR line width at various temperatures, we further concluded that the  $\text{Li}^+$  ions in the electrolyte experience a dynamic or exchange process with those in the  $\text{V}_2\text{O}_5$  cathode. Such an exchange is mediated by the  $\text{Li}^+$  ions on the surface of the  $\text{V}_2\text{O}_5$  cathode. Therefore, it is believed that the surface structure of the  $\text{V}_2\text{O}_5$  cathode electrode plays an important role in the reversibility of the  $\text{Li}^+$  ions in the rechargeable battery. When the  $\text{Li}^+$  ions are present on the surface of the  $\text{V}_2\text{O}_5$  cathode, they effectively interact with the  $\text{Li}^+$  ions both in the electrolyte and in the  $\text{V}_2\text{O}_5$  cathode, so that the  $\text{Li}^+$  ions can be inserted into or extracted from the  $\text{V}_2\text{O}_5$  cathode during the charge–discharge cycles. However, other elements such as Al in the current collector are also deposited onto the surface of the  $\text{V}_2\text{O}_5$  cathode during the charge–discharge cycles,<sup>17</sup> forming a thin coat on the surface of the cathode electrode. Apparently, such a coating does not favor the presence of the  $\text{Li}^+$  ions as no  $\text{Li}^+$  ions on the surface were observed in the over cycled state. As a result, it effectively prevents the  $\text{Li}^+$  ions from entering the cathode.

**Acknowledgment.** This research was partially supported by the U.S. Army Communications-Electronics Command and the work was largely performed at the National High Magnetic Field Laboratory supported by National Science Foundation Cooperative Agreement DMR-0084173 and the State of Florida.

### References and Notes

- (1) Baudry, P.; Lascaud, S.; Majastre, H.; Bloch, D. *J. Power Sources* **1997**, *68*, 432.
- (2) Murata, K.; Izuchi, S.; Yoshihisa, Y. *Electrochim. Acta* **2000**, *45*, 1501.
- (3) Kumai, K.; Ikeya, T.; Ishihara, K.; Iwahori, T.; Imanishi, N.; Takeda, Y.; Yamamoto, O. *J. Power Sources* **1998**, *70*, 235.
- (4) Yoshida, H.; Fukunaga, T.; Hazama, T.; Terasaki, M.; Mizutani, M.; Yamachi, M. *J. Power Sources* **1997**, *68*, 311.
- (5) Aurbach, D.; Zinigrad, E.; Teller, H.; Dan, P. *J. Electrochem. Soc.* **2000**, *147*, 1274.
- (6) Wang, H.; Jang, Y. I.; Huang, B.; Sadoway, D. R.; Chiang, Y. M. *J. Power Sources* **1999**, *81–82*, 594.
- (7) Lee, J. H.; Hong, J. K.; Jang, D. H.; Sun, Y.-K.; Oh, S. M. *J. Power Sources* **2000**, *89*, 7.
- (8) Dai, Y.; Wang, Y.; Eshkenazi, V.; Peled, E.; Greenbaum, S. G. *J. Electrochem. Soc.* **1998**, *145*, 1179.
- (9) Gerald, R. E.; Klingler, R. J.; Sandi, G.; Johnson, C. S.; Scanlon, L. G.; Rathke, J. W. *J. Power Sources* **2000**, *89*, 237.
- (10) Guerin, K.; Menetrier, M.; Fevrier-Bouvier, A.; Flandrois, S.; Simon, B.; Biensan, P. *Solid State Ionics* **2000**, *127*, 187.
- (11) Carewska, M.; Scaccia, S.; Croce, F.; Arummugam, S.; Wang, Y.; Greenbaum, S. G. *Solid State Ionics* **1997**, *93*, 227.
- (12) Stallworth, P. E.; Kostov, S.; denBoer, M. L.; Greenbaum, S. G.; Lampe-Onnerud, C. *J. Appl. Phys.* **1998**, *83*, 1247.
- (13) Pecquenard, B.; Gourier, D.; Baffier, N. *Solid State Ionics* **1995**, *78*, 287.
- (14) Delmas, C.; Cognac-Auradou, H.; Cocciantelli, J. M.; Menetrier, M.; Doumère, J. P. *Solid State Ionics* **1994**, *69*, 257.
- (15) Cocciantelli, J. M.; Menetrier, M.; Delmas, C.; Doumère, J. P.; Pouchard, M.; Hagenmuller, P. *Solid State Ionics* **1992**, *50*, 99.
- (16) Stallworth, P. E.; Johnson, F. S.; Greenbaum, S. G.; Passerini, S.; Flowers, J.; Smyrl, W.; Fontanella, J. J. *Solid State Ionics* **2002**, *146*, 43.
- (17) Moss, P. L.; Fu, R.; Au, G.; Plichta, E. J.; Xin, Y.; Zheng, J. P. *J. Power Sources* **2003**, available online 6 August 2003.
- (18) Ma, Z.; Moss, P.; Fu, R.; Au, G.; Plichta, E. J.; Zheng, J. P. *J. New Mater. Electrochem. Sys.* **2003**, submitted.
- (19) Mayne, C. L.; Alderman, D. W.; Grant, D. M. *J. Chem. Phys.* **1975**, *63*, 2514.
- (20) Fu, R.; Hu, J. Z.; Ye, C. *Acta Chimica Sinica* **1994**, *52*, 511.
- (21) Zhou, J.; Fu, R.; Hu, J. Z.; Li, L.; Ye, C. *Solid State Nucl. Magn. Reson.* **1997**, *7*, 291.
- (22) Alamo, R. G.; Blanco, J. A.; Carrilero, Y.; Fu, R. *Polymer* **2002**, *43*, 1857.
- (23) Brooks, A. A.; Cutnell, J. D.; Stejskal, E. O.; Weiss, V. W. *J. Chem. Phys.* **1968**, *49*, 1571.
- (24) Letellier, M.; Chevallier, F.; Clinard, C.; Frackowiak, E.; Rouzaud, J.; Beguin, F.; Morcrette, M.; Tarascon, J.-M. *J. Chem. Phys.* **2003**, *118*, 6038.
- (25) Carter, G. C.; Bennett, L. H.; Kahan, D. J. *Metallic Shifts in NMR. A review of the theory and comprehensive critical data compilation of metallic material. Part I*; Pergamon Press: New York, 1977.
- (26) Beuneu, F.; Vajda, P.; Zogal, O. *J. Nucl. Instrum. Methods Phys. Res.* **1998**, *B141*, 241.
- (27) Croce, F.; Brown, S. D.; Greenbaum, S. G.; Slane, S. M.; Salomon, M. *Chem. Mater.* **1993**, *5*, 1268.
- (28) Ernst, R. R.; Bodenhausen, G.; Wokaun, A. *Principles of Nuclear Magnetic Resonance in One and Two Dimensions*; Clarendon Press: Oxford, 1987.
- (29) Wagner, G.; Wüthrich, K. *Methods Enzymol.* **1986**, *131*, 307.